Sensors and Actuators A 158 (2010) 149–160

Contents lists available at ScienceDirect

Sensors and Actuators A: Physical

journal homepage: www.elsevier.com/locate/sna

Review

The high potential of shape memory alloys in developing miniature mechanical devices: A review on shape memory alloy mini-actuators

Adelaide Nespoli*, Stefano Besseghini, Simone Pittaccio, Elena Villa, Stefano Viscuso

Consiglio Nazionale delle Ricerche Istituto per l'Energetica e le Interfasi (CNR IENI), Unità Operativa di Supporto di Lecco, Corso Promessi Sposi, 29, 23900 Lecco, Italy

ARTICLE INFO

Article history:
Received 31 July 2009
Received in revised form
23 November 2009
Accepted 17 December 2009
Available online 13 January 2010

Keywords:
SMA
Smart actuators
Linear actuators
Rotational actuators

ABSTRACT

Shape memory alloys (SMAs) are a well-known class of smart materials. When subjected to certain thermal cycles, they are able to generate mechanical work by recovering a predetermined shape. Due to their high mechanical performances, their compactness and lightness, SMAs can be easily included in mechanical devices of small dimensions and used as actuating elements. There are rather few companies worldwide that deal in SMA mini-actuators; we can find, nonetheless, quite a large number of studies about them. In this paper, we illustrate the state of art of SMA mini-actuators, in the meaning of mini-modular-mechanical devices activated by SMA materials; particular attention is granted to the commercial SMA mini-actuators and to the most recent and relevant publications and patents in this field. Ferromagnetic shape memory alloys are presented as well.

Contents

1. Introduction 149
   1.1. Aim of this work 150
2. SMA mini-actuators 150
   2.1. Linear SMA mini-actuators 151
   2.2. Rotational SMA mini-actuators 153
   2.3. Ferromagnetic SMA actuators 154
   2.4. An overview on SMA and FSMA actuator patents 155
3. Discussion 156
   3.1. The ideal SMA mini-actuator 156
   3.2. Linear mini-actuators 158
   3.3. Rotational actuators 158
   3.4. Future perspective 159
4. Conclusion 159
   References 159
   Biographies 160

1. Introduction

SMAs are intermetallic compounds able to recover, in a continuous and reversible way, a predetermined shape during a heating/cooling cycle. From a microscopic point of view, this transformation consists in a transition from a crystallographic phase stable at low temperature, i.e. martensite, to a different crystallographic phase stable at high temperature, namely austenite. The critical temperatures at which transition occurs depend on the composition of the alloy, its thermo-mechanical history and the applied load. These critical temperatures indicate the onset and offset of the direct transition from austenite to martensite during cooling (M_s and M_f for martensite starting and finishing temperatures), and of the reverse transformation during which austenite is created from martensite (A_s and A_f for austenite starting and finishing temperatures) [1,2]. The forward and reverse transformations between the two phases shows a thermal hysteresis that is usually about 20–40 °C (Fig. 1).

* Corresponding author. Tel.: +39 0341 499 181; fax: +39 0341 499 214.
E-mail addresses: a.nespoli@ieni.cnr.it (A. Nespoli), s.besseghini@ieni.cnr.it (S. Besseghini), s.pittaccio@ieni.cnr.it (S. Pittaccio), e.villa@ieni.cnr.it (E. Villa), s.viscuso@ieni.cnr.it (S. Viscuso).

0924-4247/$ – see front matter © 2010 Elsevier B.V. All rights reserved.
doi:10.1016/j.sna.2009.12.020

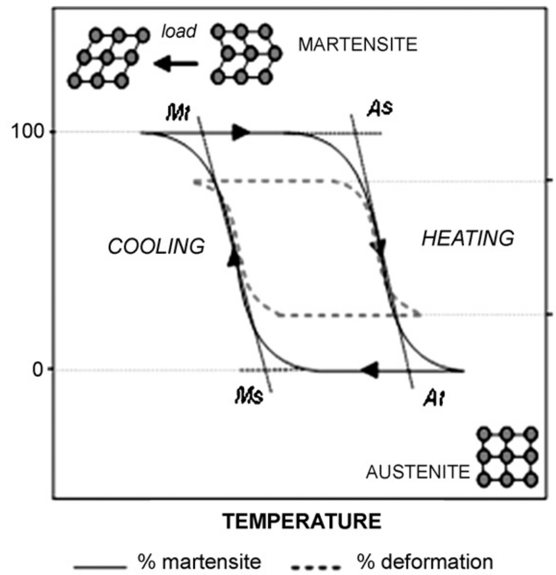

Fig. 1. Shape memory thermo-mechanical hysteresis. The phase transformation between martensite and austenite shows a thermal and a mechanical hysteresis; M_s and M_f represent the martensite start and finish temperatures while A_s and A_f are the austenite start and finish temperatures. While deformation under load is possible during cooling, shape recovery is driven by heating through the martensite–austenite phase transformation (4% is an example of working strain).

During the phase transformation SMAs are able to generate mechanical work. The force and the displacement (i.e. deformation, stroke) produced during a heating/cooling cycle are two important parameters to be considered when developing SMA actuators: they depend on the shape of the SMA element, on the chosen thermo-mechanical treatment and on the applied load.

SMA elements generally need some "training" under load for a certain number of heating/cooling cycles in order to provide a device with high reproducibility. As a consequence, the material functional characteristics will tend to follow, during every working cycle, a repeatable closed loop, such as the one in Fig. 1. The thermal and mechanical hysteresis shown in Fig. 1 is one of the factors affecting (and limiting) the precision control of SMA actuators.

Due to the ability to recover a preformed shape after a variation of temperatures, SMAs can be used also as temperature sensor.

A typical SMA actuator is generally made up of several parts: the mechanical system, the SMA element, a bias element able to restore the deformed shape of SMA element, an electric control unit and a set of fixtures used to couple the actuator with the mechanical system [3].

1.1. Aim of this work

In this paper, we present the state of art of SMA mini-actuators, constraining the meaning of this expression to mini-modular-mechanical devices activated by SMA elements and able to generate displacement (linear or angular) and force. Therefore, this analysis focuses primarily on the modular elements rather than the specific applications or solution, because modular elements can often be used for different purposes and in many different fields.

2. SMA mini-actuators

The aim of miniaturization is to develop actuators that yield high mechanical performance in a limited space; for this reason one peculiar requirement of miniaturized actuator elements is that it need be light and compact. Considering the power-to-weight ratio of different types of actuators as a function of the actuator weight (Fig. 2) it becomes evident [4,5] that SMA actuators have the highest power-to-weight ratio among light-weight technologies, which means that they have a high potential for miniaturization.

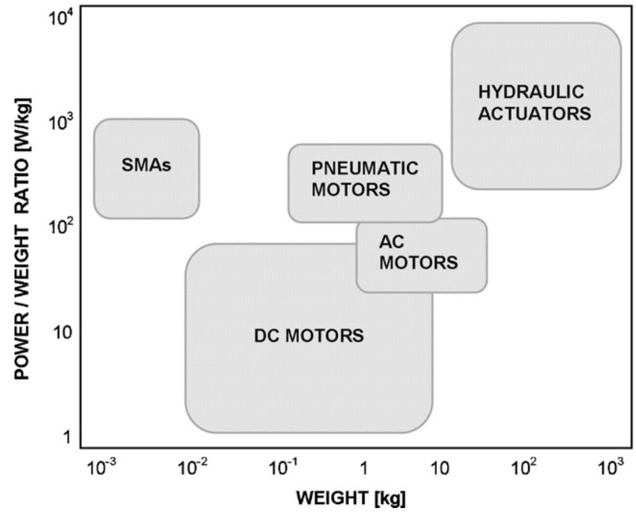

Fig. 2. Power/weight ratio vs. weight of different actuators [4,5]. Schematic representation of power density as a function of weight for the most common actuator technologies.

There are many further advantages to the use SMA materials in mini-actuators, the most relevant being the simplicity of mechanism, cleanliness, silent actuation, remotability, sensing ability, low driving voltage [4]. SMAs also have some weak points, i.e. a low energy efficiency (<10%), a strong relationship between the strain operation range and fatigue life [4], quite a low response speed and a non-linear behaviour (Fig. 1).

The SMA element has often a spring or a wire shape and is coupled with a bias element, that could be a SMA component too. In general, the SMA element is linked with an output shaft that transfers the movement outside the device (see Fig. 3 as an example).

There are rather few companies worldwide that deal in SMA mini-actuators. In our research, we found only one company that deals exclusively with this kind of devices, i.e. the Miga Motor Company. Instead, the published scientific literature comprises quite a large number of studies that propose SMA materials as actuator elements in miniaturized modular mechanical devices.

Fig. 3. Two way action actuator [6]. A SMA spring and a stainless steel spring are mounted in a holder working one against the other. When the SMA spring is heated it recovers its initial shape pushing the holder and deforming the stainless steel spring; during cooling the stainless steel spring retracts the holder deforming the SMA spring.

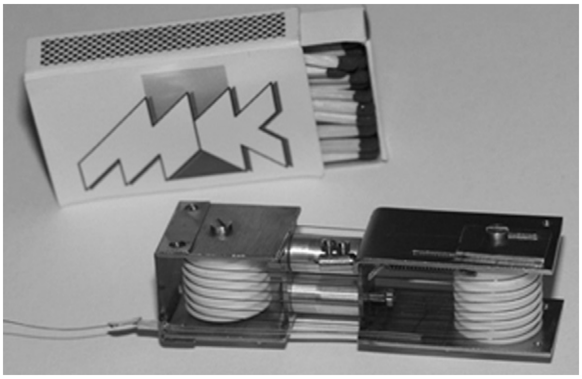

Fig. 4. Drive module by Jansen et al. [7]. 1000 mm long SMA wire with a diameter of 0.2 mm is wound on two sets of seven pulleys. In the large displacement mode this actuator can reach a displacement of 30 mm and a force of 4 N, while in the high force mode it can develop a displacement of 2.2 mm and a force of 56 N.

In the next pages we present the most recent and relevant publications concerning SMA mini-actuators, grouped according to whether they provide linear or rotational motion; commercial SMA mini-actuators are presented as well. An overview on the most recent SMA mini-actuator patents is presented too. Comparisons and comments are presented in Section 3.

2.1. Linear SMA mini-actuators

Jansen et al. developed a linear actuator (Fig. 4, Fig. 16) used as a drive module in an angular positioning mini-actuator [7]. The drive module uses a 1000 mm long SMA wire with a diameter of 0.2 mm, wound on two sets of seven pulleys. A bias spring is fixed to one end of the SMA wire in such a way that when the applied load exceeds its maximum force, the electric circuit is opened and the SMA wire stops contracting. The bias spring maximum load can be adjusted by a screw. The drive module can be used in two different modes: as a large displacement or as a high force actuator. In the first mode, the displacement of the free end of the SMA wire is chosen as output parameter; in this case, the drive module can reach a displacement of 30 mm and a force of 4 N. In the second mode the two ends of the SMA wire are fixed and the force is applied directly on the frame; in this case the actuator can reach a force of 56 N and a displacement of 2.2 mm. The dimensions of the module are $75 \times 20 \times 20\,\text{mm}^3$.

Strittmatter and Gümpel proposed a SMA actuator for the activation of a hydraulic valve [8]. Fig. 5 shows a schematic representation of the operation principle and the prototype of the actuator. When an electric current is applied, SMA wires contract and cause a movable flange to shift; the flange possesses a shaft that transfers the movement outside the closing screw. When energy supply is interrupted, an outside spring, not shown in figure, pulls the shaft back and the flange to the bottom of the closing screw. Tests were carried out on a hydraulic testing bench at a hydraulic pressure of 200 bar with an oil temperature of 24 °C; two NiTi wires of 201 μm in diameter are considered. With a maximum current of 2.5 A ($24\,V_{max}$) the actuators show a stroke of 0.8 mm against a force of 98 N, provided by the spring. Actuation time is set to 0.4 s while revert motion completes in 3 s.

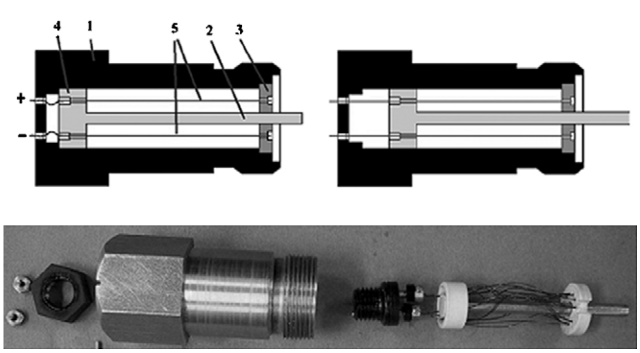

Fig. 5. SMA actuator by Strittmatter and Gümpel [8]. Linear device composed of (1) closing screw, (2) shaft, (3) guide plate, (4) flange, (5) SMA wires; the actuator shows a maximum stroke of 0.8 mm against a force of 98 N.

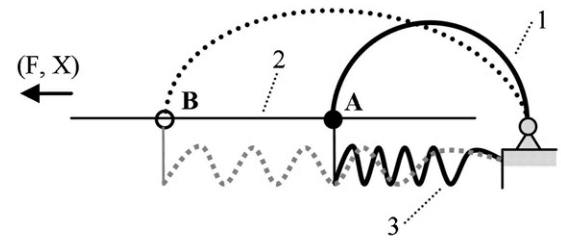

Fig. 6. Scheme of the linear actuator generating force in one direction presented by Pulnev et al. [9]. (1) Shape memory bending force element; (2) output element; (3) bias steel spring. When heated, the SMA element unbends forcing the output element to shift from point A to point B and deform the steel spring; during cooling the steel spring forces the SMA element to bend and the output element to return to point A.

Pulnev et al. proposed two kinds of linear actuators (for one and two directions of movement) based on SMA bending elements made of CuAlNi alloy single crystal [9]. Fig. 6 displays the scheme of the actuator generating force in one direction: heating causes the SMA element to straighten, thus forcing the output element to shift from point A to point B and deforming the steel spring. During cooling the steel spring forces the SMA element to bend again and the output element to return to point A. The maximum displacement calculated for this actuator is 9.7 mm with an output force of 69 N. No experimental tests were reported.

Fig. 7 presents the scheme of the actuator generating force in two directions: heating causes the first SMA element to straighten and forces the output element to shift from point A to point B. The second SMA element is thus deformed. When the second SMA element is heated the first SMA element is forced to bend back and the output element to return to point A. Also for this kind of actuator no mechanical either experimental tests were carried out.

This functioning principle that uses a SMA bending element is also used in the rotational actuators developed by Priadko et al. [10].

Haga et al. proposed a mini-actuator used in a Braille display. This is made up of two counteracting compression SMA springs [11,12], which have a diameter of 1.6 mm and are able to develop an extending force of 10 gf. Using a current of 200 mA, this actuator is able to reach a stroke of 10 mm. The actuator operates as follow: when a SMA spring is heated by Joule's effect, the connected pin shifts and is attracted by an iron plate magnetised by a permanent magnet. Therefore, the position of the pin is maintained even if the electric current is set off, allowing a reduction in power consumption (Fig. 8).

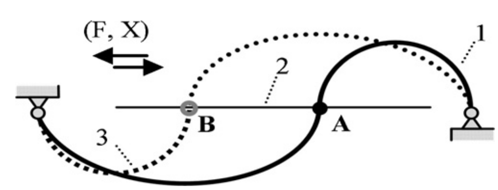

Fig. 7. Scheme of the linear actuator generating force in two directions presented by Pulnev et al. [9]. (1 and 3) Shape memory bending force elements; (2) output element. During heating, the first SMA element unbends forcing the output element to shift from point A to point B and deform the second SMA element; when the second SMA element is heated the output element returns to point A deforming the first SMA element.

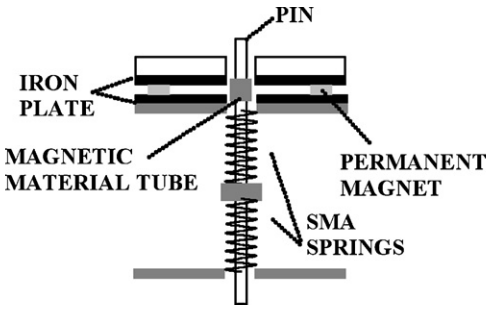

Fig. 8. Schematic representation of the actuator by Haga and co-workers [11,12]. Two antagonist compression SMA springs when alternatively activated move a pin that is able to maintain a particular position thanks to tube which can be attracted by an iron plate magnetised by a permanent magnet.

Velázquez et al. developed a linear actuator used in a tactile binary information display [13] made up by two bias springs. It has a diameter of 1.5 mm, a length of 45 mm, a weight of 150 mg and is able to develop a pull force of 320 mN (Fig. 9). Forced-air convection is used to accelerate the cooling time. Using a current of 1.3 A, this actuator is able to reach a stroke of 3 mm.

Donnellan suggested an improvement to the mini-linear-actuator developed by Starsys Research and Applied Physics Laboratory (ALP) [14]. The original ALP actuator consists in a travel pin that is moved by a SMA wire with a diameter of 0.076 mm coupled with a bias steel spring (Fig. 10).

Donnellan replaced the SMA wire with a SMA compression spring in order to obtain a larger stroke. Fig. 11 shows the solution proposed by Donnellan: a steel spring is placed inside the SMA compression spring, long 7.6 mm and with a diameter of 6 mm; the SMA wire has a length of about 160 mm and a diameter of 0.58 mm. The end loops of the steel spring are forced inside two plates in order to keep the SMA spring compacted; during heating the SMA spring recovers its shape deforming the steel spring. The final stroke reached by Donnellan's actuator is about 7 mm with an activation time longer than 1 s.

Colli et al. [15] propose a linear SMA actuator able to vary the air inflow for internal combustion engines, improving gas combustion and leading to higher fuel economy and engine performances. Fig. 12 shows a CAD model of the actuator and a photo of the prototype. In this actuator two SMA spring sets work as mutual antagonists, producing the linear movement of an output shaft; the actuation force is 35 N while the maximum shaft displacement is 20 mm.

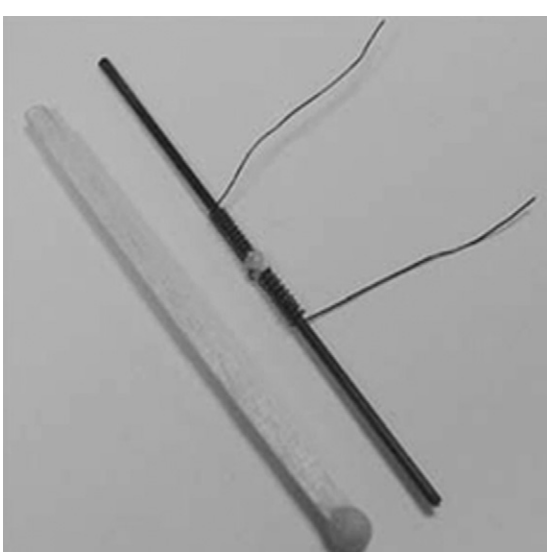

Fig. 9. Mini-actuator prototype by Velázquez et al. used in a tactile binary information display ©2005 IEEE. The actuator is composed by two bias SMA springs that move a pin.

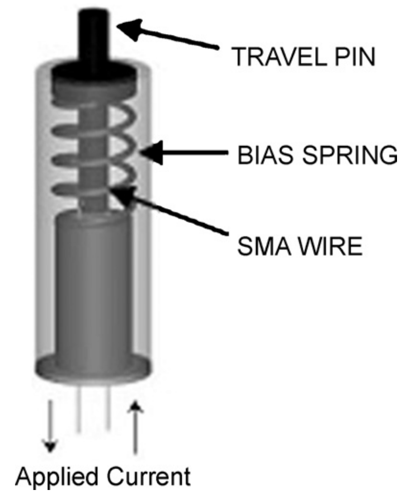

Fig. 10. The Starsys Research and Applied Physics Laboratory mini-actuator [14]. A travel pin is moved by a SMA wire that works against a bias spring.

Elwaleed et al. developed a SMA beam actuator (Fig. 13) able to amplify the SMA actuator strain using elastic beams [16,17,18]. In this work, a 150 mm long SMA wire with a diameter of 0.7 mm is eccentrically constrained on a flexible beam into six segments. This configuration leads to an amplification of the wire deformation: the system provides displacements up to 20 mm, i.e about 280% larger than the displacement offered by the unconstrained wire. When temperature rises up to and beyond the A_F temperature, the SMA wire contracts and the beam deflects. After cooling the beam acts as a bias element deforming back the SMA wire. The actuator is composed of two such beams connected to two plates (one fixed and another one able to move) and a shaft connected to the moving plate, that transfers the movement outside the device. The dimensions of the actuator are: $150 \times 45 \times 35\,mm^3$.

Pittaccio et al. developed a mini-linear-actuator employed in a device for the repetitive and passive mobilization of a flaccid ankle [19]. This actuator ($150 \times 20 \times 15\,mm^3$) is made of an alu-

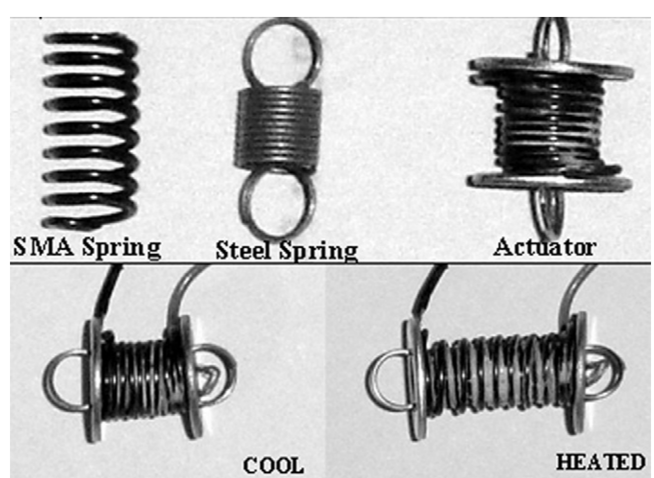

Fig. 11. Donnellan's improvement to the Starsys Research and Applied Physics Laboratory mini-actuator [14]. A SMA compression spring coupled with a steel spring is used to generate stroke; the steel spring is put inside the SMA spring and keeps the SMA spring deformed. The main improvement is in the output stroke.

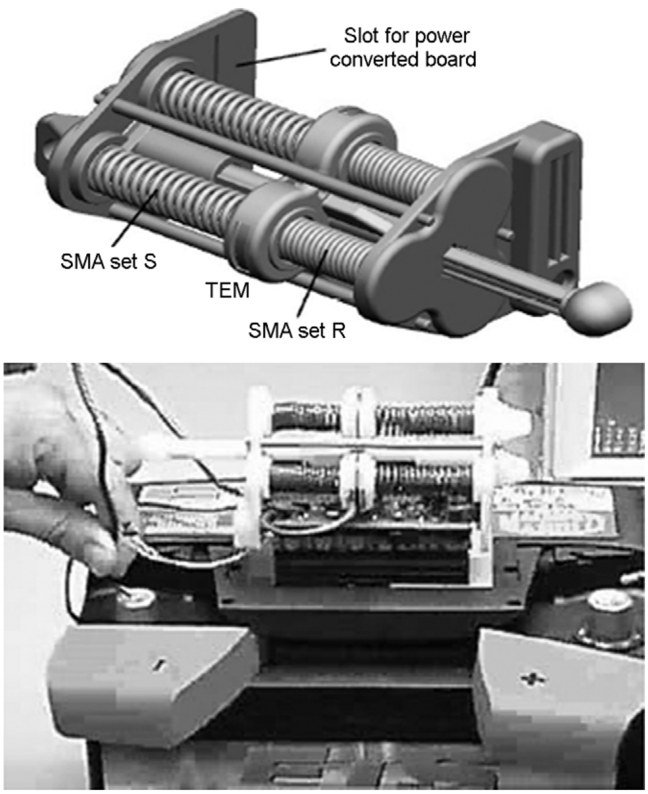

Fig. 12. CAD model and photo of the SMA actuator by Colli et al. ©2006 IEEE. Two SMA spring sets, working as mutual antagonists, produce the linear movement of an output shaft.

minium cartridge wherein a 250 cm long NiTi wire with a diameter of 250 μm is pulled back and forth between two sets of mini-pulleys; a pseudoelastic spring is linked to the NiTi wire moving end in order to maintain it stretch (Fig. 14). With a supplied current of 0.7 A this actuator generates a maximum displacement of 8 cm (i.e. 3.2% of strain) under a load of 8.83 N in 7 s. Cooling is achieved by natural convection; initial shape is restored in 30 s. Movement is transferred outside the cartridge by an inextensible thread fixed to the NiTi wire moving end.

Miga Motor Company produces a large variety of modular SMA linear actuators. These devices are able to provide stroke-lengths up to 1.27 cm and forces up to 20 N. The DM01 series, Mobi, Dash and Migaone actuators have an A_s of 75 °C, an A_f of 110 °C and a

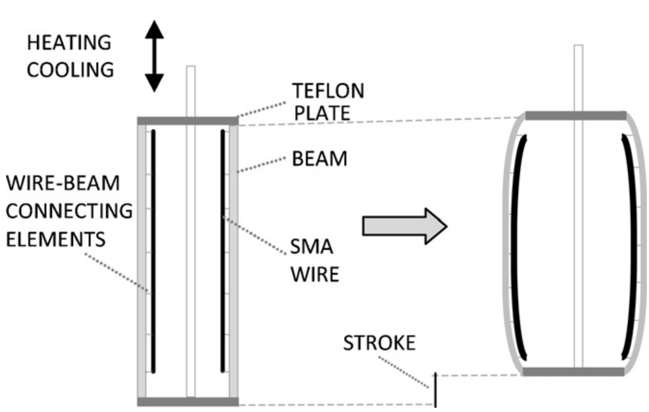

Fig. 13. Schematic representation of the actuator by Elwaleed et al. [16,17,18]. A SMA wire is constrained on a flexible beam by seven connecting elements, providing a displacement of the movable plate of about 20 mm. During movement the beams bend by the pulling action of the wires.

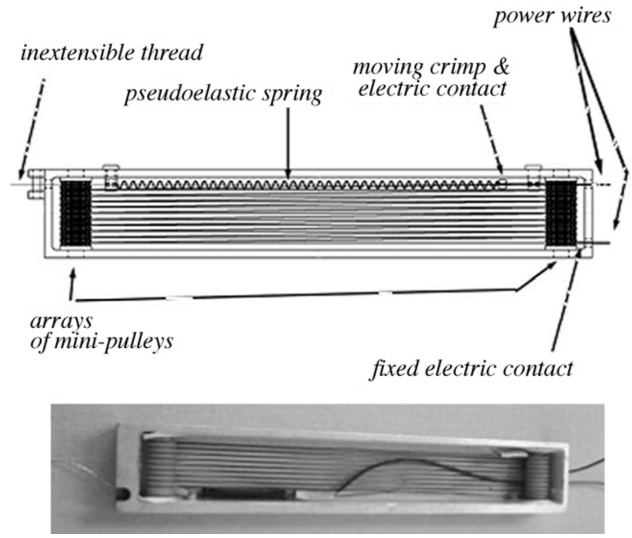

Fig. 14. Schematic representation and prototype of the mini-linear-actuator by Pittaccio et al. [Fig. 2 – with kind permission of Springer Science and Business Media]. 250 cm long NiTi wire is wounded on two sets of pulleys; the wire is maintained stretched by a pseudoelastic spring. Under a load of 8.83 N the actuator reaches a displacement of 8 cm.

critical temperatures of 150 °C. The martensite finishing temperature, M_f, is 60 °C. An external bias force is needed in order to return an un-powered actuator to its rest position when it is under load. MIGAONE™ actuator is made of five segments of SMA wire with a diameter of 0.3 mm; MOBI™ and DASH™ actuators are made of 3 segment of SMA wire. Table 1 shows all Miga Motor SMA linear actuators with details on stroke, output force and geometrical dimensions [20].

2.2. Rotational SMA mini-actuators

Park et al. developed several mini-rotary-actuators using SMA wires [21]. A simple joint actuator able to achieve an angular bi-directional deflection of 60° by using two embedded SMA wires having a diameter of 100 μm, is used to develop a more complex mechanisms that transform a stepping rotational motion into a continuous rotational motion. The rotary joint moving in one direction causes the continuous rotation of a ratchet wheel and a pawl lets the ratchet wheel to move only in one direction. The measured torque for this actuator is 0.08 N mm.

Pöhlau and Meier propose a high-torque drive activated by six pairs of SMA wires [22]. The device is composed of an internal flexible gear wheel (called the Flexring), six pairs of SMA wires fixed radially inside the Flexring, an external rigid gear wheel. The Flexring has external teeth while the external gear wheel has internal teeth; the two gear wheels interfere with each other due to the coupling of the teeth on either side. The activation of a pair of SMA wires produces a deformation in the Flexring; the radial

Table 1
Miga Motor SMA linear actuators [20].

Actuator	Stroke (mm)	Output force (N)	Dimensions ($l \times w \times t$ mm^3)
DM01-10	12.7	9	79.4 × 21.5 × 7.3
DM01-12	12.7	12	79.4 × 21.5 × 7.3
DM01-15	12.7	20	79.4 × 21.5 × 7.3
MOBI™	3.2	4.5	12.7 × 28.6 × 2
DASH4™	5.8	7	24.1 × 68.3 × 2.88
MIGAONE™	9	11	72.9 × 34.8 × 2.88
NM70-Super	4	0.7	6 × 34.7 × 5.32
NForce™	11.4	71	–

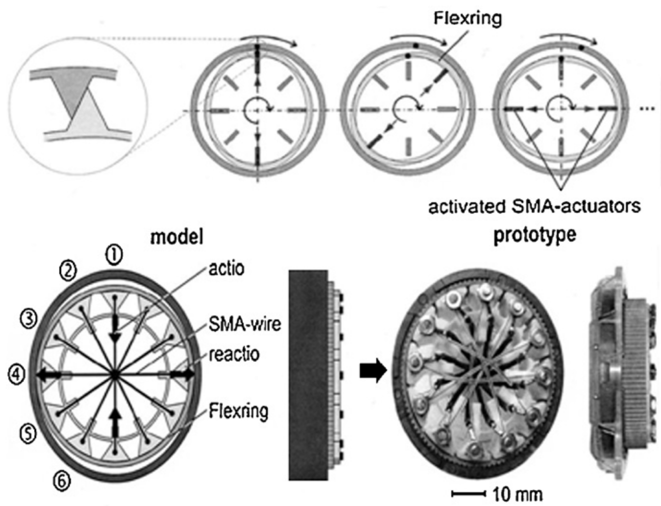

Fig. 15. Functional principle and prototype of the drive system by Pöhlau and Meier [22]. Six pairs of SMA wires are positioned radially inside a flexible gear wheel that has external teeth. Activating the pairs of SMA wires one after the other generates the intermittent rotation of a second wheel that has internal teeth which interfere with the flexible ring ones.

force produced by the SMA wires is transformed into a tangential force at the tooth flanks and generates a torque. Activating the pairs of SMA wires one after the other generates an intermittent rotational motion of the external gear wheel. The functional principle is shown in Fig. 15. SMA wires have a diameter of 0.3 mm, the external diameter of the entire actuator is 55 mm, its length is 15 mm. The maximum driving torque is about 2.5 N m. It is important to notice that Pöhlau actuator uses the SMA element not to produce the primary actuator stroke.

Jansen et al. suggest an angular positioning mini-actuator made up of different modules [7]: two drive modules activated by SMA wires (Fig. 4), a gear module connected to the output shaft and the drive modules, a brake module and a snap module both activated by SMA wires used as a braking mechanism, a casing module and a sensor-control module (Fig. 16). Using a 0.2 mm SMA wire, each drive module can provide a maximum displacement of about 30 mm and a force of up to 4 N. The output SMA wire of the two drive modules are connected to a pulley inside the gear module, producing the rotation of an output shaft connected to the gear pulley. The maximum angular range is 180°, while the maximum output

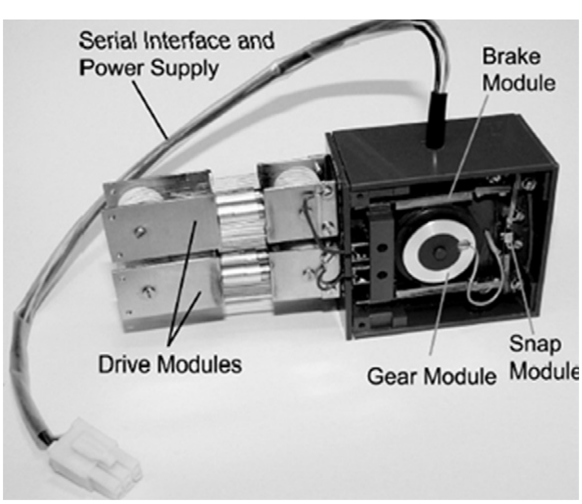

Fig. 16. Prototype of the positioning actuator by Jansen et al. [7]. Two drive modules generate the rotation of an output shaft by 180° under a torque of 4 N cm.

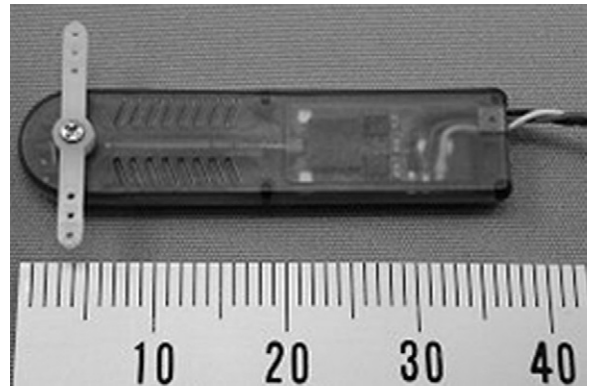

Fig. 17. SmartServo actuator RC-1 [25,26]. The actuator is able to turn 30° right and left achieving a torque of 1.5 N mm.

torque is 4 N cm. No mechanical test is presented. Dimensions are: 70 × 67 × 40 mm^3.

Sharma et al. studied a poly-phase motor based on SMA wire [23,24]. The three phase one has the dimensions of 150 × 150 × 20 mm; it is made up of three SMA wires (diameter 0.35 mm and length 120 mm) in series with a linear spring, which is in turn fixed to a cam and to an adjustable anchor. In order to reduce the size of the motor, three pulleys are used to fold back the SMA wire. During activation, the SMA elements are forced-air cooled so as to abate concentrated heating in proximity of the connection between them and the other parts of the motor. Under a torque of 2 kg mm this motor makes a rotation of 360° in 5 s.

Toki Corporation Biometal® division deals in SMA actuators. In Fig. 17 is presented their SMA rotary actuator, the SmartServo RC-1, that is able to turn bi-directionally its arm across 60° in 0.25 s (30° right and left each side). The SMA element has a wire shape with a diameter of 60 μm and a length of 28 mm, and is connected to a bias spring [25,26]. Operating in a range of temperature between 0 °C and 40 °C, it achieves a torque of 1.5 N mm consuming an average power of 0.15 W. The actuator dimensions are: 38 × 9 × 3 mm^3.

Miga Motor SMA rotational actuators are presented in Table 2, with details on stroke, output torque and dimensions [20].

2.3. Ferromagnetic SMA actuators

Ferromagnetic shape memory alloys (FSMAs) change shape when subjected to a mechanical stress and/or to a magnetic field [27,28,29]. Due to their fast response time (less than a millisecond) and to the high strain (over 10%), FSMA represents an optimum candidate in developing actuators. NiMnGa is the best-working and best-known FSMA [30,31,32,33].

Mini-modular-mechanical devices activated by a FSMA element are not as common as the ones activated by a SMA component. We only found one company dealing in FSMA mini-actuators, i.e. AdaptaMat Ltd.

Fig. 18 shows the most recent actuator developed by AdaptaMat; it is composed by two NiMnGa elements of 20 × 2.5 × 1.0 mm each and is pre-stressed with a spring (that can be changed to suit the desired application). The maximum stroke it can reach is 0.7–0.8 mm with an output force of 5–7 N. The dimensions are about 80 × 80 × 70 mm^3.

Table 2
Miga Motor SMA rotational actuators [20].

Actuator	Stroke (°)	Output torque (N mm)	Dimensions ($l \times w \times t$ mm^3)
RS-125-CE	60	2	12.7 × 55.25 × 7.5
RS-70-CE	60	1.2	12.7 × 55.25 × 7.5
NM70R	60	–	–

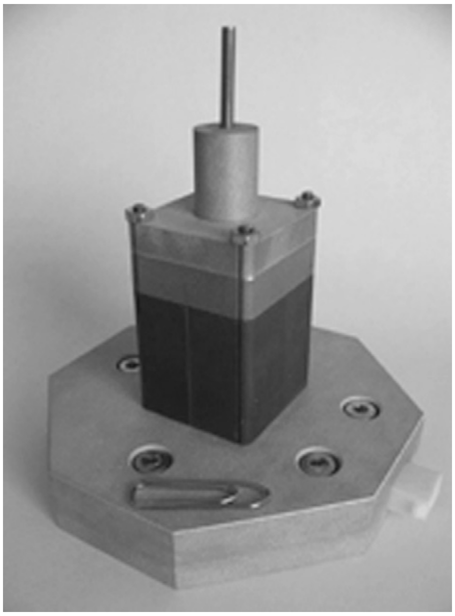

Fig. 18. AdaptaMat actuator [34]. The actuator can reach a stroke of 0.7–0.8 mm with an output force of 5–7 N.

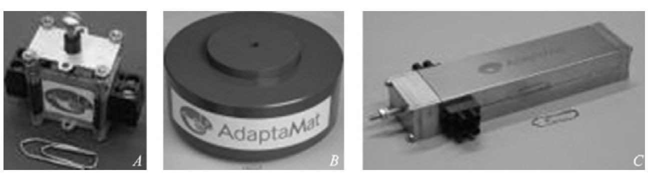

Fig. 19. AdaptaMat actuators [29,34]. Previous product lines of AdaptaMat: (A) the A06-3 actuator that reaches a stroke of 0.6 mm; (B) the A-1 2000 actuator achieves a strain of 2.8% under a pressure of 1.25 MPa; (C) the last linear actuator provided a maximum output force of 1 N.

Previously AdaptaMat used to produce different actuators shown in Fig. 19. The A06-3 actuator achieves the maximum stroke (about 0.6 mm) at 200 Hz and has the blocking force of 2.5 N; it reaches a stroke of 3% in 0.2 ms. The A-1 2000 actuator has an iron core and can achieve strains of 2.8% at a stress of 1.25 MPa.The last one is a linear actuator that generates a linear motion; the average shaft speed (with no load) is 40 mm/s and the provided force is 1 N [34].

Murray [28] and Du Plessis et al. [35,36] developed two more prototypes of FSMA actuator; in particular, Du Plessis' actuator uses two FSMA antagonist elements in order to control a position of a valve spool.

2.4. An overview on SMA and FSMA actuator patents

This section lists some of the most recent and relevant patents about SMA actuators, particularly focussing on those patents published within the last five years. Because of the lack of any geometrical dimensions reported for these actuators, we decided to exclude them from the Discussion, as no reasonable comparisons with the other devices could be made.

Takahashi invented a SMA linear actuator [37] composed by a SMA wire, two moving bodies and two bias springs positioned in a cylinder. When the SMA wire is heated, a first moving body is shifted against a bias spring and a second bias spring elongates and pushes a second moving body against the first moving body. When cooling, the first bias spring pushes the first moving body against the second moving body and the second bias spring shortens.

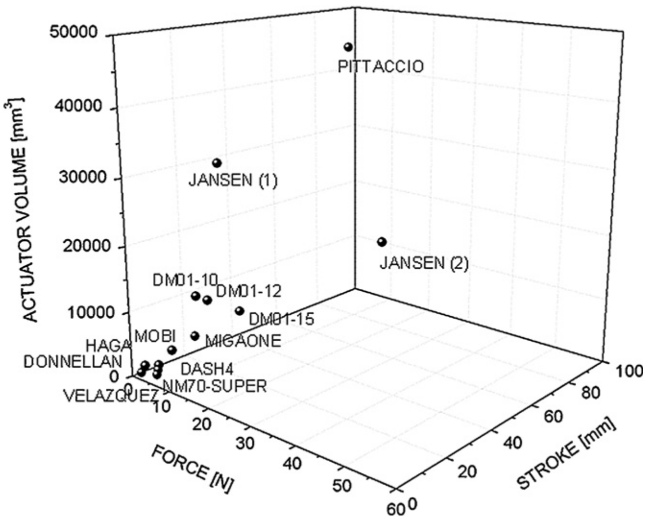

Fig. 20. Stroke, force and actuator volume characteristics of linear actuators. Relationship between the main mechanical parameters, i.e. stroke and force, of the linear actuators as a function of their volumes.

Garscha et al. invented a turn-actuator with a tensile element made of SMA [38]. Two SMA elements are fixed to a rotational element in such a way that when the first SMA element is activated it generates a rotation of the rotational element in one direction and when the second SMA element is activated and the first SMA element is deactivated the rotational element rotates in the opposite direction. A third SMA component acting against a spring shifts a slider in order to move the rotational element away from a brake element.

Apolonio P. Yson et al. invented a shape memory alloy linear actuator [39] composed of a couple of SMA members in such a way that during heating some members increase their length and the other members get shorter. The SMA members have a tubular shape and are set coaxially providing a telescopic extension.

Butera studied [40] an actuator made of a SMA wire and a series of means that can increase the load applied on the SMA wire when temperature increase, increasing the transformation temperatures of the SMA wire. The means are compound by a bias spring and by a SMA element.

Asada et al. invented a SMA actuator system for the coordination of both gross and fine movement [41]. The system is composed by a series of SMA wires each of which is divided into many segments controlled separately, forming a two-dimensional array.

Gummin et al. invented several linear shape memory alloy actuators [42] that show a multi-links connections and several rotational actuators [43] that includes SMA wires positioned in a series of helical grooves obtained in a cylindrical bobbin.

Jacot et al. invented a rotary actuator [44] composed of a SMA torque tube and a bias superelastic return spring connected with each other at their ends, and a heating element whose activation causes the torque tube to get into its austenitic phase. Under cooling the superelastic spring deforms the torque tube to its starting configuration.

Taya et al. invented a torque actuator incorporating shape memory alloy composites [45]. An FSMA member is activated by a magnetic trigger and produces a torque that rotates another member. The FSMA member could be a pure ferromagnetic element or a composite compounds of a ferromagnetic part and a SMA part.

Taya et al. also invented a linear actuator based on ferromagnetic shape memory alloy composites [46]. A hybrid magnetic trigger composed by an electromagnet and a permanent magnet activates an FSMA spring that is attracted by the permanent magnet providing a linear displacement.

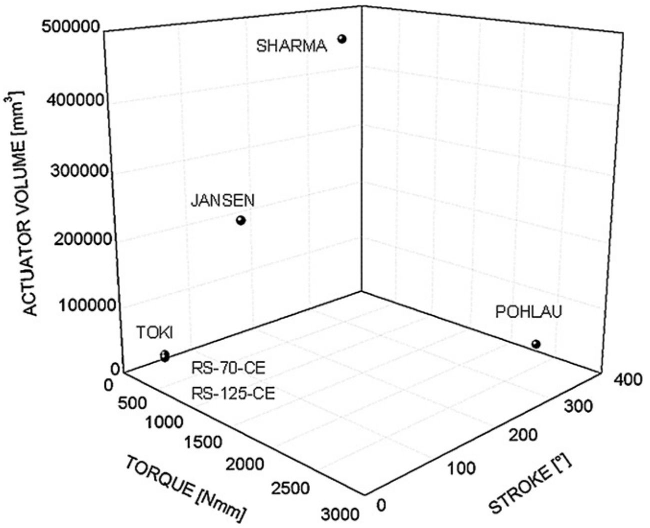

Fig. 21. Stroke, torque and actuator volume characteristics of rotational actuators. Relationship between the main mechanical parameters, i.e. stroke and torque, of the rotational actuators as a function of their volumes.

3. Discussion

In the previous paragraphs we presented several linear and rotational SMA mini-actuators derived from the published literature and from the market. The drive to the development of these actuators was their final use. This means that the urge to meet certain specific functional requirements, severely affected the designers' choices regarding the shapes and volumes the actuators should possess in order to produce predefined strokes and output forces. Incidentally, some solutions to specific problems produced devices of relatively small size and high energy density, that can be treated as mini-actuators. In this paper, we do not intend to give any judgement about how adequately any device meets its declared goals, but on the contrary, disregarding applications, we rather set about to produce an *ex post* classification, trying to gain more insight on the overall potential of SMA for generating mini-modular-actuators.

Figs. 20 and 21 show the relationship between output force or torque, stroke and volume of the linear and rotational actuators we previously presented. The NForce actuator as well as those by Pulnev, Strittmatter, Colli, and Park had to be excluded, because no geometrical dimension was reported; the Elwalleed actuator was also left out as output force was not declared. The theoretically "best mini-actuator" should have force, stroke and volume values such that it lie in the bottom-right corner of the two graphs shown in Figs. 20 and 21. In particular, we believe that a "true" mini-actuator ought to have a volume of about 1 cm^3. From this pictures it is evident that there is a physical limitation in fabricating a mini-actuator that satisfies such requirements: actuators that have a small volume do not reach a high force or a high stroke value and, on the other hand, actuators that reach a high force or a high stroke do not fit into small volumes.

In order to compare the mechanical performance of all the actuators presented in this work and having in mind that "true" mini-actuators must be small, we decided to normalize the stroke, the output force or torque and the mechanical work they produce by their occupied volume. Therefore, for each actuator we define four functional parameters, i.e. a stroke-to-volume ratio, S_R; a force-to-volume ratio for linear actuators, F_R; a torque-to-volume ratio for rotational actuators, T_R; and a work-to-volume ratio, W_R:

$$S_R = \frac{\text{Stroke}}{\text{Volume}} \quad F_R = \frac{\text{Force}}{\text{Volume}} \quad T_R = \frac{\text{Torque}}{\text{Volume}} \quad W_R = \frac{\text{Stroke Force}}{\text{Volume}} \tag{1}$$

The purpose of such a normalization is to create some parameters that permit to compare the mechanical performance of different actuators independently of their geometrical dimensions. In particular, functional parameter W_R represents the specific mechanical work and directly accounts for the miniaturization efficiency.

The four functional parameters are influenced by the working environment conditions. In particular there is one main factor that strongly affects the mechanical performance of an SMA actuator, that is to say the working temperature. In fact, if the temperature reaches a value between M_f and A_f (which are both dependent on the particular applied load) the actuator cannot recover completely its starting condition and consequently the maximum stroke the device can reach is modified. In a high temperature environment, we can also observe that the heat transfer to the surrounding medium is reduced, resulting in a longer cycling time for the actuator; on the other hand, in a low temperature environment, the heat transfer to the surrounding medium is improved, resulting in a shorter cycling time, however coupled with a greater power expense to achieve the transformation temperature A_f. If the working temperature is above A_f, the alloy has a pseudoelastic behaviour and cannot be used in developing modular-actuators as defined in this work. For all these reasons, there seems to exist a most indicated working temperature, which lies just below M_f: it was assumed in this work that actuator designers would have chosen in an appropriate manner the SMA material for their own devices.

Of course the performance of any actuator cannot really match the mechanical output of the sheer SMA element, because a certain amount of energy will be lost, e.g. due to the friction between the mechanical parts. In order to quantify the losses in mechanical performance, we shall compare each functional parameter calculated using Eq. (1) for every real actuator with the values obtained for an *ideal mini-actuator* composed only by an SMA element.

3.1. The ideal SMA mini-actuator

We defined as an *ideal SMA mini-actuator* the actuator composed only by an SMA NiTi wire having a volume of 1 cm^3. For this SMA wire we shall consider a working strain of 5%, a volume density of 6.5 g/cm^3 and a transformation latent heat of 24 J/g [47]. The *ideal SMA mini-actuator* needs an energy equal to the latent heat in order to transform from the austenite into the martensite phase and vice versa; no energy is lost during phase transformation, because no friction occurs. This means that we are taking the latent heat as representing the asymptotical upper limit of the energetic yield of a real linear mini-actuator, apart from the intrinsic loss connected to the transformation hysteresis.

For each mini-actuator, when possible, we calculated the volume ratio, V_R, defined as the ratio between the SMA element volume and the actuator volume and compared it with the *ideal SMA mini-actuator* one, that is equal to 1 (Fig. 22).

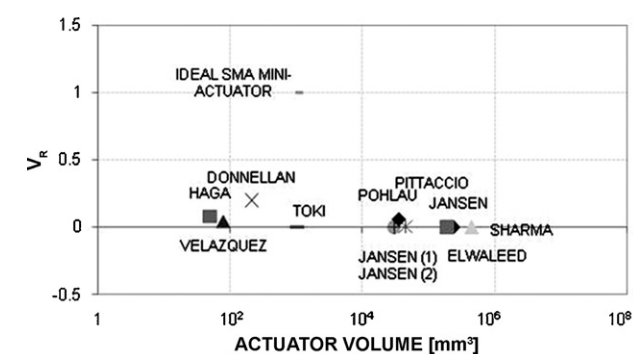

Fig. 22. V_R vs. actuator volume for all actuators. The ratios between the SMA element volume and the actuator volume, V_R, are compared and ordered as a function of each actuator volume for all linear and rotational actuators.

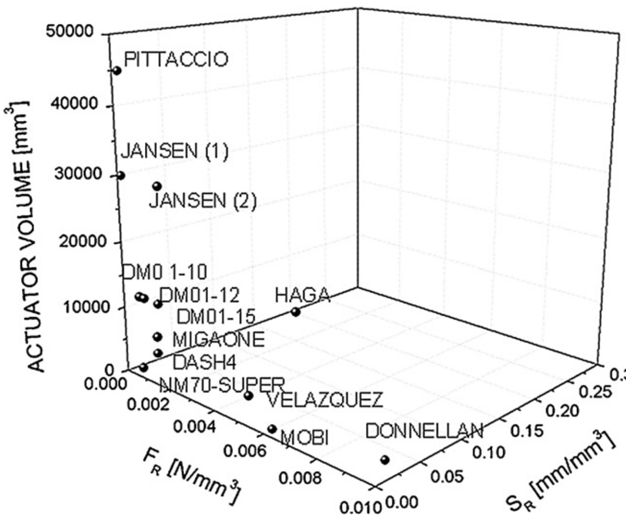

Fig. 23. F_R vs. S_R vs. actuator volume of linear actuators. Comparison between the main mechanical parameters of the linear actuators, i.e. force and stroke, normalized by the actuator volume as a function of the actuator volume.

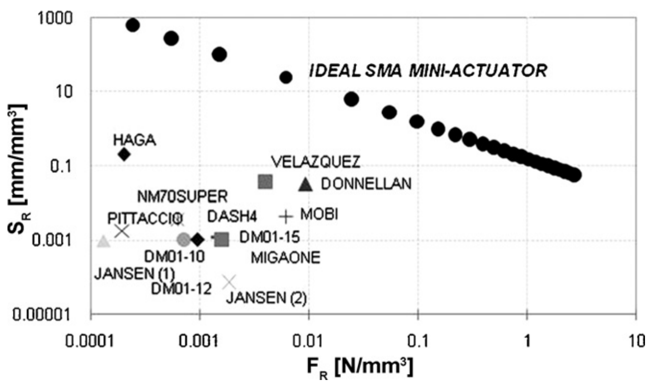

Fig. 24. S_R vs. F_R of linear and *ideal* SMA actuators in bilogarithmic scale. Comparison between the actuator stroke normalized by the actuator volume of the linear and the *ideal* actuators as a function of the actuator force normalized by the actuator volume.

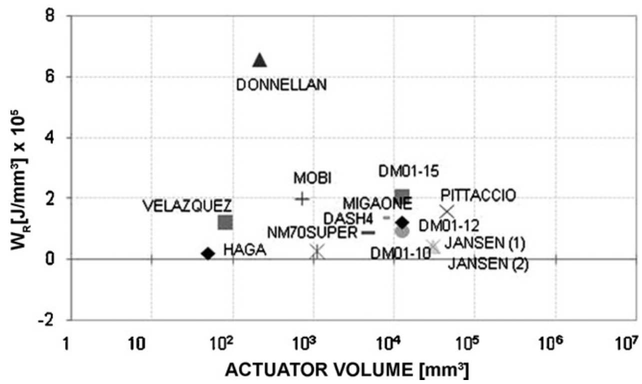

Fig. 26. W_R vs. actuator volume for linear actuators. Comparison of the specific mechanical work as a function of the actuator volume, W_R, for the linear actuators.

Donnellan's actuator is the only one having a V_R slightly closer to the value found for the *ideal* mini-actuator one. This occurs because it is composed of very few mechanical parts, its volume being almost totally occupied by the SMA element.

It is important to underline that among all SMAs, there are few commercial candidates we can choose as the point of reference in developing mini-actuators: NiTi, CuZnAl and CuAlNi. NiTi is the overall best aspirant, having the highest thermo-mechanical performances [48]. For this reason we considered the characteristic parameters of NiTi (volume density and latent heat) as the ones to be used to define the *ideal mini-actuator.* We do not exclude a priori the use of any other alloy instead of NiTi; the recommendation is to substitute the enthalpy and the volume density of NiTi with

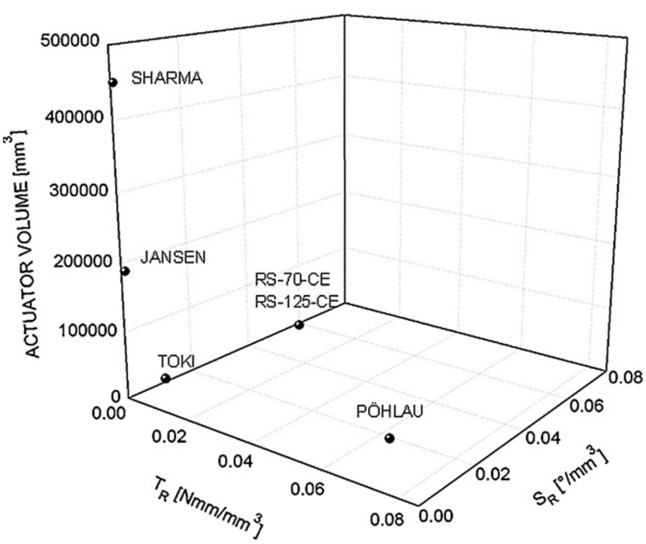

Fig. 27. T_R vs. S_R vs. actuator volume for rotational actuators. Relationship between the main mechanical parameters of the rotational actuators, i.e. torque and stroke, normalized by the actuator volume as a function of the actuator volume.

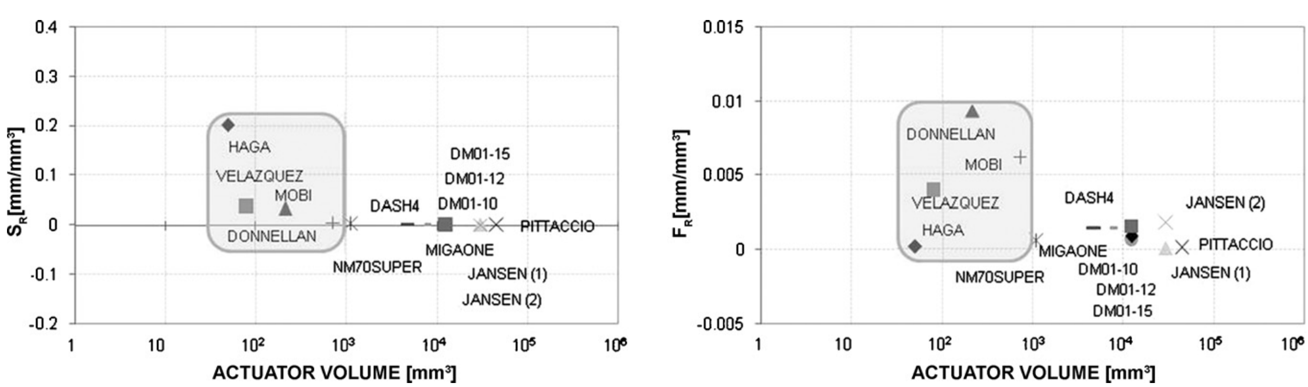

Fig. 25. S_R vs. actuator volume and F_R vs. actuator volume of linear actuators. Comparison between stroke-to-volume and force-to-volume ratios normalized by the actuator volume of the linear actuators as a function of the actuator volume. The grey areas contain the actuators with volume less than 1 cm^3.

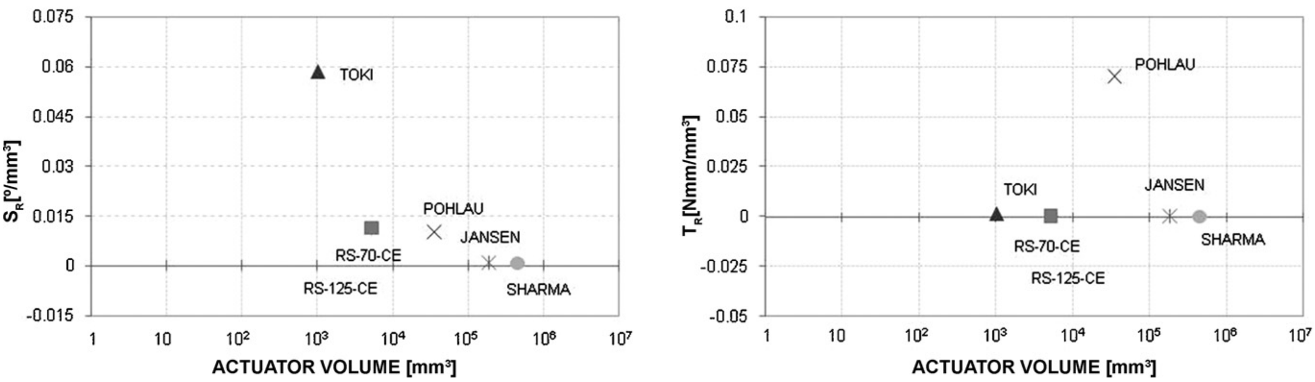

Fig. 28. S_R vs. actuator volume and T_R vs. actuator volume for rotational actuators. Comparison between stroke-to-volume and torque-to-volume ratios normalized by the actuator volume of the rotational actuators as a function of the actuator volume.

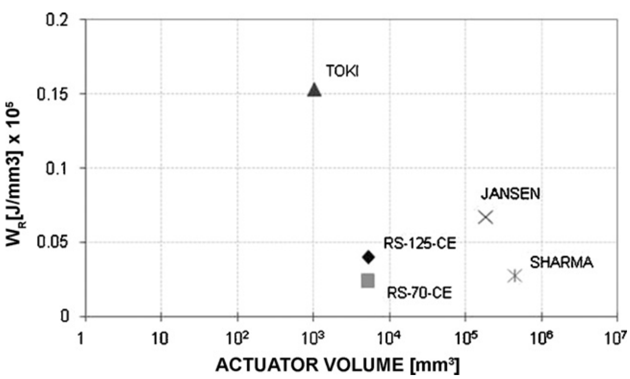

Fig. 29. W_R vs. actuator volume for rotational actuators. Comparison of the specific mechanical work, W_R, as a function of the actuator volume of the rotational actuators.

the ones for the new alloy. Moreover, we also have to consider that the *ideal mini-actuator* based on an alloy different from NiTi, will perform worse than NiTi in terms of maximum deformation. For example, alloys such as NbRu and TaRu reach deformations up to 1.5–2%; ZrCu, CoNiAl (single crystal), NiTiPd and NiTiPt could maximally be deformed up to 3–4%. CuAlNi (single crystal) have a similar deformation capabilities as NiTi [49], i.e. around 8.

3.2. Linear mini-actuators

Fig. 23 shows the relationship between S_R, F_R and the volume for the linear actuators we considered. In this figure we can see that all real actuators fall in one and the same part of the F_R–S_R-actuator volume space. In particular, in the F_R–S_R plane we can plot an equilateral hyperbola with the asymptotes equal to the coordinate axes, that divides this plane in two parts: a part that comprises all the actuators and a part with no actuators. This equilateral hyperbola represents the mechanical upper limit in developing mini-actuators and it is well represented by the *ideal SMA mini-actuator*. This equilateral hyperbola is derived by the following equation:

$$H = \frac{\text{Stroke Force}}{\text{Volume}} \tag{2}$$

where H is the latent heat of the phase transformation between austenite and martensite. Combining Eqs. (1) and (2) we obtain the equilateral hyperbola equation in Cartesian coordinates in the F_R–S_R plane:

$$S_R = \frac{H}{\text{Volume}} \frac{1}{F_R} \tag{3}$$

Fig. 24 shows the S_R–F_R values of each linear actuators and of the equilateral hyperbola in bilogarithmic scale. The equilateral hyperbola equation is calculated for a discrete number of *ideal* SMA wires of different diameter and length, using data listed in Section 3.1 and Eq. (3); in the bilogarithmic scale the equilateral hyperbola has a straight line trend.

Among all actuators, Donnellan's best approximates the values of functional parameters for an *ideal SMA mini-actuator*. The actuators by Haga, Velazquez, Donnellan and Mobi have a volume less than 1 cm^3 and present S_R and F_R values higher than the others (see also Fig. 25).

In doing such a comparison, is important to note that some real mini-actuator presents a bias component which limits both the stroke and the force of the single SMA element; on the other hand the *ideal SMA mini-actuator* does not work against any opponent force. Therefore, those real mini-actuators presenting two groups of elements working one against the other, may have S_R and F_R real values actually somewhat higher than the ones shown in Fig. 24.

Donnellan's actuator also has the highest miniaturization efficiency, see Fig. 26, that is about 3–4 times greater than the one of the other linear mini-actuators. The SMA element of Haga's, Velazquez's and Donnellan's actuators have a spring shape, demonstrating that spring is the best shape when developing SMA mini-actuators.

3.3. Rotational actuators

Fig. 27 shows the relationship between T_R, S_R, and the volume of the rotational actuators we previously presented, except Park's one, as no geometrical dimensions were found for that.

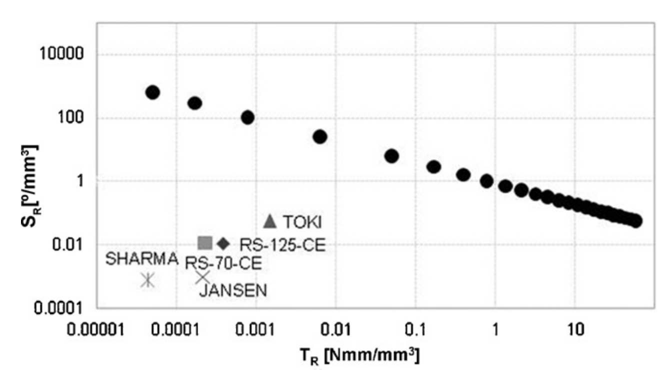

Fig. 30. S_R vs. T_R of rotational and *ideal* SMA actuators in bilogarithmic scale. Comparison between the actuator stroke normalized by the actuator volume of the rotational and the *ideal* actuators as a function of the actuator torque normalized by the actuator volume.

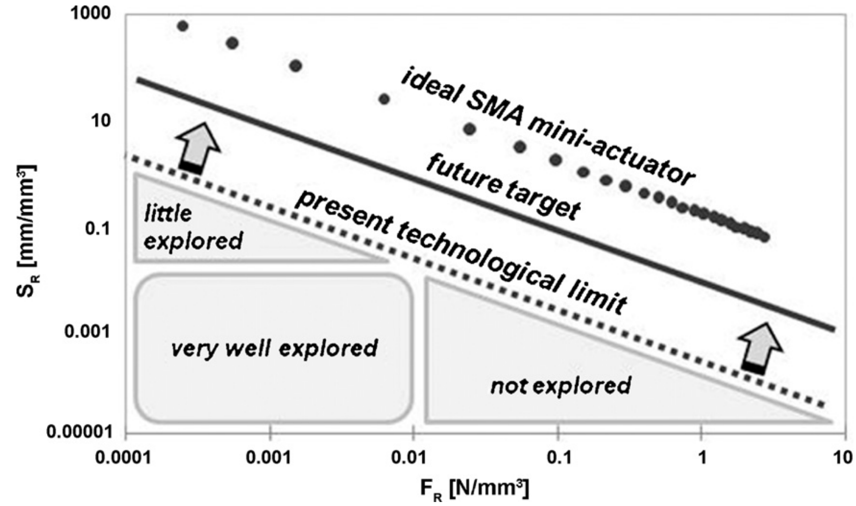

Fig. 31. Future perspective on SMA mini-actuators. Comparison between the current technological limit and the *ideal* characteristics of SMA mini-actuators.

In Fig. 28 we can see that Toki's actuator is the one with the smallest volume (just over 1 cm^3); it also has the highest S_R value but a low T_R. Pöhlau's actuator has the highest T_R value, but in this case the SMA element is not used to produce the primary actuator stroke.

As we did for the linear actuators, we can define an *ideal mini-actuator* also for the rotational ones. This actuator is based on the SMA ideal element as defined in Sections 3.1 and 3.2; the generated ideal torque is equal to the product of the ideal F_R and the ideal lever arm *b*. We can imagine that during rotation the SMA wire binds around an ideal shaft which has the diameter equal to the lever arm. If we assume that the SMA wire upper external fibers must not exceed 5% of deformation, we can establish a mathematical relationship between the lever arm and the diameter of the SMA wire *d* by using equation:

$$0.05 = \frac{2d}{2b + a} \quad (5)$$

Solving Eq. (5) and substituting it in the equation of the ideal torque, we can plot in the S_R-T_R plane an equilateral hyperbola which in the bilorathmic plane has a straight line trend. Among all rotational actuators, excluding Pöhlau's one, Toki's actuator is the one showing the best miniaturization efficiency and the one that get closer to the ideal behaviour, as shown in Figs. 29 and 30.

3.4. Future perspective

As regards linear actuators, in the S_R-F_R plane we can trace a straight line through the location of Donnellan's actuator and parallel to the one representing the *ideal SMA mini-actuator* characteristics. This line is the current virtual technological limit in the exploitation of the SMA materials for developing mini-actuators. We can then distinguish three areas (see Fig. 31) below this limit: almost all the actuators we presented lie within the central area, with small S_R and F_R. A second area, with large S_R and small F_R, is very little explored as yet (i.e. only Haga's actuator fall into this region). The third area is currently unexplored. A possible future target is to investigate this third area by developing SMA mini-actuators with mechanical performance that suit high F_R and low S_R values. A more complex and demanding future goal is to try and get closer to the *ideal SMA mini-actuator* mechanical performance, shifting the virtual technological limit line nearer to the *ideal* one.

4. Conclusion

Miniature SMA-activated devices do not have a huge commercial market as yet; there are however quite a large number of studies and patents about them. SMA compactness leads to a large versatility in the final choice for a device shape; however, the final use and the specific functional requirements (force and stroke) strongly affect both the final shape and the volume of the actuator.

In this paper, we presented several linear and rotational SMA mini-actuators, with the intention to study, by comparing their mechanical performance, the high potential of shape memory alloy in developing miniature mechanical devices.

The actuator volume is an important parameter to consider when comparing the mechanical behaviour of different mini-actuators; normalizing the main mechanical dimensions by the actuator volume allowed us to make comparisons independently of geometrical dimensions and verify how far the mechanical performance of a specific mini-actuator is from that of the *ideal* one, i.e. from the characteristics of an actuator composed only by the SMA element without any other mechanical part.

By comparing the mechanical performance of published SMA linear mini-actuators, we found that the spring shape grants the highest mechanical performance to the SMA element and the smallest geometrical dimensions to the miniaturized actuators. The performance of rotational actuators is far less affected by SMA element shape, but it can be said that this type of devices tend to have an overall volume larger than the linear ones.

The performance SMA mini-actuators is about two orders of magnitude smaller than the *ideal* figure. This means both that there is a sort of limitation in fabricating mini-actuators that reasonably approximate the *ideal* one and that there is a great potential for further optimization. New technical applications and greater commercial opportunities for these devices could descend from a better exploitation of SMA properties and more innovative design.

References

[1] H. Funakubo, Shape Memory Alloys, Gordon & Breach Science Publishers, 1984.
[2] K. Otsuka, C.M. Wayman, Shape Memory Materials, Cambridge University Press, 1998.
[3] M. Mertmann, G. Vergani, Design and application of shape memory actuators, Eur. Phys. J. Special Top. 158 (2008) 221–230.
[4] K. Ikuta, Micro/Miniature Shape Memory Alloy Actuator, IEEE-ICRA, 1990.
[5] C. Mavroidis, Development of advanced actuators using shape memory alloys and electrorheological fluids, Res Nondestr Eval 14 (2002) 1–32.
[6] T. Ishii, Combinations and applications of bias method, in: Proceedings on SMST, 2007.

[7] S. Jansen, J. Breidert, E.G. Welp, Positioning actuator based on shape memory wires, in: ACTUATOR 2004, 9th International Conference on New Actuators, 2004.
[8] J. Strittmatter, P. Gümpel, Shape memory actuator for hydraulic valve, in: ACTUATOR 2004, 9th International Conference on New Actuators, 2004.
[9] S. Pulnev, I. Vahhi, A. Priadko, A. Rogov, Miniature linear actuators based on Cu–Al–Ni shape memory single crystals, in: Proceedings on SMST, 2004.
[10] A. Priadko, S. Pulnev, I. Viahhi, Actuator based on Cu–Al–Ni single crystals, in: Proceedings on SMST, 2000.
[11] Y. Haga, W. Makishi, K. Iwami, K. Totsu, K. Nakamura, M. Esashi, Dynamic braille display using SMA coil actuator and magnetic latch, Sens. Actuators A 119 (2005) 316–322.
[12] Patent No: US 2008/0227060 A1.
[13] R. Velázquez, E. Pissaloux, J. Szewczyk, Miniature shape memory alloy actuator for tactile binary information display, in: Proceedings on IEEE-ICRA, 2005.
[14] Q.A. Donnelan, Design and testing of linear shape memory alloy actuator, Final Report, National Science Foundation – Research Experience for Undergraduates, 2005.
[15] M. Colli, A. Bellini, C. Concari, A. Toscani, G. Franceschini, Current-Controlled Shape Memory Alloy Actuators for Automotive Tumble Flap, IECON, 2006.
[16] A.K. Elwaleed, N.A. Mohamed, M.J. Mohd NoR, M.M. Mohd, A new concept of a linear smart actuator, Sens. Actuators, A 123 (2007) 244–249.
[17] A.E. Elwaleed, N.A.N. Mohamed, M.J. Mohd Nor, M.F. Ma Tahir, Geometrical modelling of SMA beam actuator, in: Seminar on Engineering Mathematics, 2008.
[18] A.K. Elwaleed, Nik A. Mohamed, M.J. Mohd Nor, M.M. Mohd, A new method for actuating parallel manipulators, Sens. Actuators A 147 (2008) 593–599.
[19] S. Pittaccio, S. Viscuso, M. Rossini, L. Magoni, S. Pirovano, E. Villa, S. Besseghini, F. Molteni, SHADE: a shape memory-activated device promoting ankle dorsiflexion, J. Mater. Eng. Perform. (2009).
[20] Miga Motor Company, http://www.migamotors.com.
[21] B.H. Park, M. Shantz, F. Prinz, Scalable rotary actuators with embedded shape memory alloy, Proceedings on SPIE 4327 (2001) 78–87.
[22] F. Pöhlau, H. Meier, Extremely compact high-torque drive with shape memory actuators and strain wave gear Wave Drive®, in: ACTUATOR 2004 9th International Conference on New Actuators, 2004.
[23] S.V. Sharma, M.M. Nayak, N.S. Dinesh, Modelling, design and characterization of shape memory alloy-based poly-phase motor, Sens. Actuators A 147 (2008) 583–592.
[24] S.V. Sharma, M.M. Nayak, N.S. Dinesh, Shape memory alloy based motor, Sādhanā 33 (Part5) (2008) 699–712.
[25] Toki Corporation, http://www.toki.co.jp/biometal.
[26] D. Homma, S. Uemura, F. Nakazawa, Functional anisotropic shape memory alloy fiber and differential servo actuator, in: Proceedings on SMST, 2007.
[27] V.A. Chernenko, S. Besseghini, Ferromagnetic shape memory alloys: Scientific and applied aspects, Sens. Actuators A 142 (2008) 542–548.
[28] S.J. Murray, Ferromagnetic shape memory alloys, principles and applications, in: Proceedings on SMST, 2004.
[29] J. Tellinen, I. Suorsa, A. Jääskeläinen, I. Aaltio, K. Ullakko, Basic properties of magnetic shape memory actuators, in: Proceedings on ACTUATOR 2002, 8, 2002, p. 566.
[30] V.A. Chernenko, V.V. Kokorin, Ni_2MnGa as a new ferromagnetic ordered shape memory alloy, in: Proceedings on ICOMAT-92, 1993, pp. 1205–1210.
[31] S. Besseghini, M. Pasquale, F. Passaretti, A. Sciacca, E. Villa:, NiMnGa polycrystalline magnetically activated shape memory alloy: a calorimetric investigation, Scripta Mater. 44 (2001) 2681–2687.
[32] A. Sozinov, A.A. Likhachev, N. Lanska, K. Ullakko, Giant magnetic field-induced strain in NiMnGa seven-layered martensitic phase, Appl. Phys. Lett. 80 (2002) 1746–1748.
[33] P. Müllner, V.A. Chernenko, G. Kostorz, Large magnetic field-induced deformation and magneto-mechanical fatigue of ferromagnetic Ni-Mn-Ga martensites, Mater. Sci. Eng. A387-389 (2004) 965–968.
[34] http://www.adaptamat.com/.
[35] A.J. Du Plessis, A.W. Jessiman, G.J. Muller, M.C. van Schoor, Latching valve control using ferromagnetic shape memory alloy actuators SPIE Smart Structures and Materials, 5054, 2003.
[36] Patent No: US 2004/020692 A1.
[37] Patent No: US 2009/0013684 A1.
[38] Patent No: US 2008/0271559 A1.
[39] Patent No: US 7,464,548 B2.
[40] Patent No: WO/2009/000859.
[41] Patent No: US 7,188,473 B1.
[42] Patent No: US 7,256,518, B2.
[43] Patent No: US 7,021,055 B2.
[44] Patent No: US 7,037,076 B2.
[45] Patent No: US 2007/0289301 A1.
[46] Patent No: US 2007/0236314 A1.
[47] G. Wang, X.X. Jiang, D. Nikanpour, Measurement of specific heat, latent heat and phase transformation temperatures of shape memory alloys, High Temperatures-High Press. 37 (2008) 91–107.
[48] W Huang, On the selection of shape memory alloys for actuators, Mater. Des. 23 (2002) 11–19.
[49] G.K. Kannarpady, A. Bhattacharyya, S. Pulnev, I. Vahhi, The effect of isothermal mechanical cycling on Cu–13.3Al–4.0Ni (wt%) shape memory alloy single crystal wires, J. Alloys Compd. 425 (2006) 112–122.

Biographies

Adelaide Nespoli. She was born in 1974 in Mariano Comense, Italy. She graduated in Bioengineering (Technological and Industrial course of studies) in 2004 at Politecnico di Milano presenting a thesis dealing with a new calibration procedure of distortion product otoacoustic emissions. She is presently working as researcher at the Italian National Research Council's Institute for Energetics and Interphases (CNR IENI – Lecco) focusing on Shape Memory Alloys and their applications in actuators, also collaborating with several companies in developing new smart devices.

Stefano Besseghini. He was born in Tirano (Italy) in 1966. He graduated in Physics in 1992 with a thesis on micromemory effects in NiTi shape memory alloys. He obtained his master degree in Science and Technology of Materials at University of Milan (1995). Main interests are in the field of martensitic transformations and Shape Memory Alloys. At present he works as a researcher at the Italian National Research Council's Institute for Energetics and Interphases (CNR IENI – Lecco).

Simone Pittaccio. He was born in 1975 in Milan, Italy. He read Mandarin receiving a Bachelor Degree in 1996. He studied Bioengineering at Politecnico di Milano being awarded a M.Sc. in 2000. He carried out his doctoral research at University College London and Great Ormond Street Hospital (Ph.D. in 2004). He has been serving since 2004 as research fellow and then as researcher at the Italian National Research Council's Institute for Energetics and Interphases focusing on Shape Memory Alloys in neuromuscular rehabilitation. He published several papers on subjects ranging from computational fluid dynamics to biomechanics, applied materials science and neuroscience.

Elena Villa. She was born in 1969 in Monza (Italy). She graduated in Physics in 1995 at University of Milano with a thesis on IR and Raman spectroscopic study of conducting polymers. She obtained her master degree in Science of Polymers at Politecnico of Milano in 1997. At present she works as a researcher at the Italian National Research Council's Institute for Energetics and Interphases (CNR IENI-Lecco); her main field of work is the physical characterization of Shape Memory Alloys and innovative alloys in general. She also collaborates in different projects for the technological transfer to industrial companies.

Stefano Viscuso. He was born in 1980 in Como, Italy. He studied Bioengineering at Politecnico di Milano being awarded a M.Sc. in 2005. Since 2006, he is working on developing new applications of shape memory alloys in neuromuscular rehabilitation at the Italian National Research Council's Institute for Energetics and Interphases, serving as research fellow. He published several papers on biomechanics, applied materials science and neuroscience.